This article was downloaded by:
On: *28 January 2011*
Access details: *Access Details: Free Access*
Publisher *Taylor & Francis*
Informa Ltd Registered in England and Wales Registered Number: 1072954 Registered office: Mortimer House, 37-41 Mortimer Street, London W1T 3JH, UK

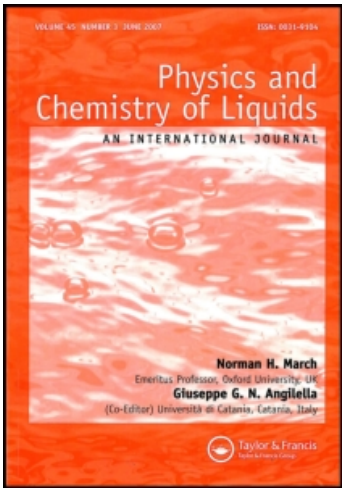

Physics and Chemistry of Liquids
Publication details, including instructions for authors and subscription information:
http://www.informaworld.com/smpp/title~content=t713646857

Lennard-Jones Elastic Moduli by Liquid Structure Integral Equations and Molecular Dynamics Computer Simulations

D. M. Heyes[a]
[a] Department of Chemistry, Royal Holloway and Bedford New College, University of London, Egham, Surrey, UK

To cite this Article Heyes, D. M.(1989) 'Lennard-Jones Elastic Moduli by Liquid Structure Integral Equations and Molecular Dynamics Computer Simulations', Physics and Chemistry of Liquids, 20: 2, 115 — 130
To link to this Article: DOI: 10.1080/00319108908036398
URL: http://dx.doi.org/10.1080/00319108908036398

PLEASE SCROLL DOWN FOR ARTICLE

Full terms and conditions of use: http://www.informaworld.com/terms-and-conditions-of-access.pdf

This article may be used for research, teaching and private study purposes. Any substantial or systematic reproduction, re-distribution, re-selling, loan or sub-licensing, systematic supply or distribution in any form to anyone is expressly forbidden.

The publisher does not give any warranty express or implied or make any representation that the contents will be complete or accurate or up to date. The accuracy of any instructions, formulae and drug doses should be independently verified with primary sources. The publisher shall not be liable for any loss, actions, claims, proceedings, demand or costs or damages whatsoever or howsoever caused arising directly or indirectly in connection with or arising out of the use of this material.

Phys. Chem. Liq., 1989, Vol. 20, pp. 115-130
Reprints available directly from the publisher
Photocopying permitted by license only

© 1989 Gordon and Breach Science Publishers Inc.
Printed in Great Britain

LENNARD-JONES ELASTIC MODULI BY LIQUID STRUCTURE INTEGRAL EQUATIONS AND MOLECULAR DYNAMICS COMPUTER SIMULATIONS

D. M. HEYES

Department of Chemistry, Royal Holloway and Bedford New College, University of London, Egham, Surrey TW20 OEX, UK.

(Received 3 January 1989)

The infinite frequency shear modulus, G_∞, and compressional modulus, K_∞, of the Lennard-Jones, LJ, fluid have been determined over essentially the whole phase diagram at densities below the solid-fluid coexistence line using PY, HNC, and Rogers and Young (RY) closures of the Ornstein-Zernike relation. At low density PY is best at reproducing simulation G_∞, and K_∞, whereas close to the coexistence line, above the critical temperature, the RY closure is best and is remarkably accurate. Agreement is poorest for all three closures below T_c in the liquid phase.

KEY WORDS: Shear and bulk infinite frequency modulus, Lennard-Jones, integral equations, computer simulations.

Downloaded At: 08:33 28 January 2011

1 INTRODUCTION

The infinite frequency shear, G_∞, and bulk moduli, K_∞, of single component fluids play a central role in interpreting their viscoelastic behaviour[1]. The values of G_∞ and K_∞ have been determined by Molecular Dynamics computer simulation and parameterised for a simple fluid such as the Lennard-Jones fluid[2,3]. However no such thorough study of the available integral equation methods has been made, to examine how satisfactory they are in reproducing these moduli. The infinite frequency moduli can be derived directly from the structure of the fluid at the level of the pair radial distribution function, $g(r)$. The Ornstein-Zernike equation is a path to $g(r)$[4,5],

$$h(r) = c(r) + \rho \int d\underline{r} c(|\underline{r} - \underline{r}'|) h(\underline{r}'), \tag{1}$$

where ρ is the number density, $c(r)$ is the direct correlation function and the total correlation function, $h(r)$, is,

$$h(r) = g(r) - 1, \tag{2}$$

Defining $\gamma(r)$,

$$\gamma(r) = h(r) - c(r), \tag{3}$$

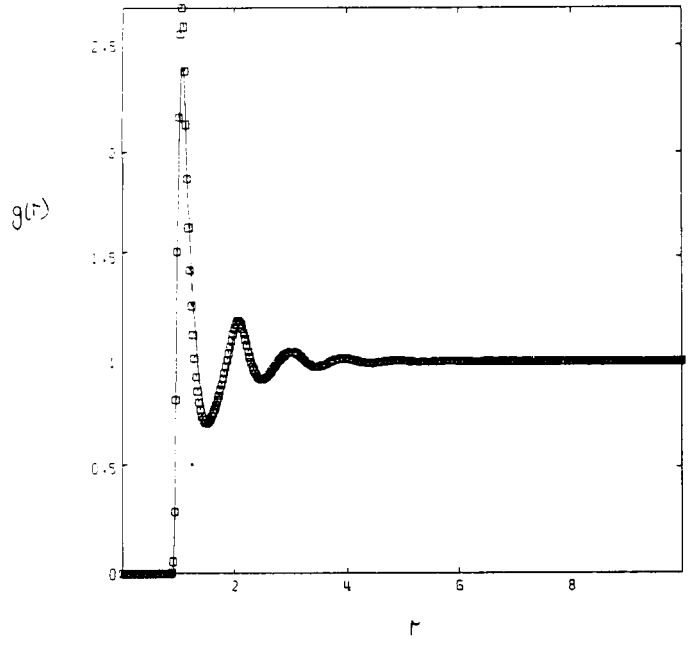

Figure 1 Comparison between the pair radial distribution functions generated by *MD* (solid lines) and *PY* (squares) at $T = 1.06$ and $\rho = 0.731$. $N = 256$ in the MD simulations.

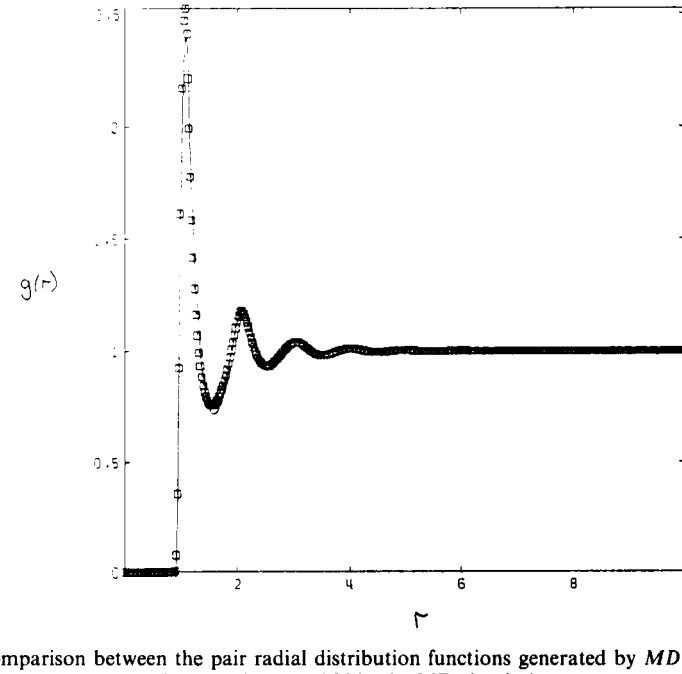

Figure 2 Comparison between the pair radial distribution functions generated by *MD* (solid lines) and *HNC* (squares) at $T = 1.06$ and $p = 0.731$. $N = 256$ in the MD simulations.

Downloaded At: 08:33 28 January 2011

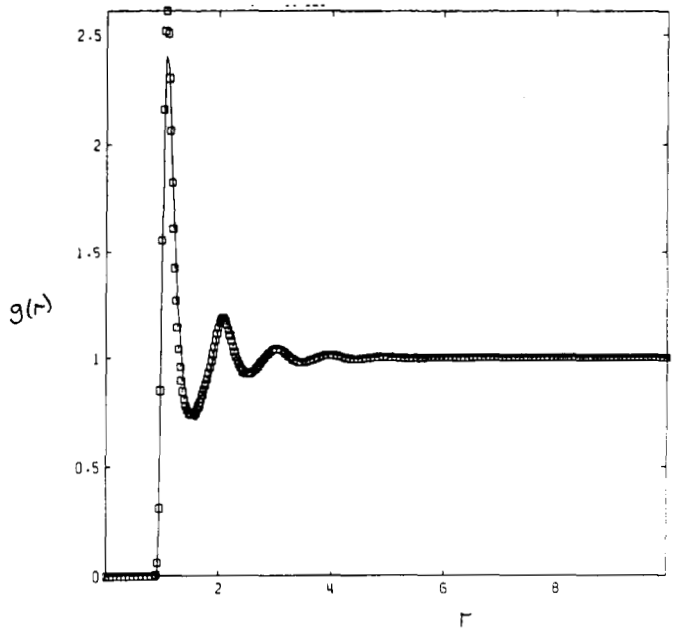

Figure 3 Comparison between the pair radial distribution functions generated by *MD* (solid lines) and *RY* (squares) at $T = 1.06$ and $\rho = 0.731$. $N = 256$ in the MD simulations.

Downloaded At: 08:33 28 January 2011

then Eq. (1) can be solved with an arbitrary closure relation. We will consider three possibilities.

Percus-Yevick, PY

$$\begin{aligned} c(r) &= (1 + \gamma(r))(\exp(-\beta\phi(r)) - 1), \\ &= (1 + \gamma(r))\exp(-\beta\phi(r)) - 1 - \gamma(r) \end{aligned} \tag{4}$$

where $\beta = 1/(k_B T)$ and $\phi(r)$ is the interatomic potential. This closure has been the subject of numerous treatments of the Lennard-Jones fluid[5–14]. Therefore, using Eqs. (2) and (3) we have,

$$g(r) = (1 + \gamma(r))\exp(-\beta\phi(r)). \tag{5}$$

Hypernetted Chain[4]

$$c(r) = \exp(-\beta\phi(r) + \gamma(r)) - 1 - \gamma(r), \tag{6}$$

and

$$g(r) = \exp(-\beta\phi(r) + \gamma(r)). \tag{7}$$

Rogers-Young, RY[15]

$$c(r) = \exp(-\beta\phi(r))\left(1 + \frac{\exp(\gamma(r)f(r)) - 1}{f(r)}\right) - 1 - \gamma(r), \tag{8}$$

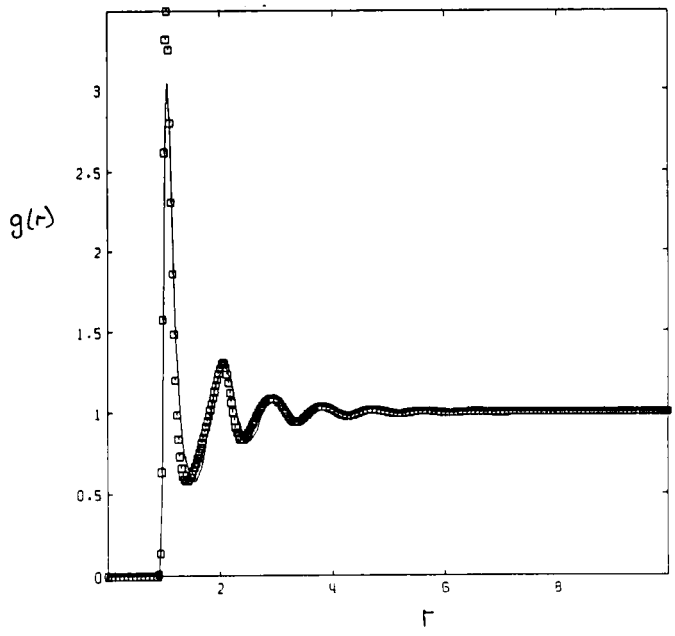

Figure 4 Comparison between the pair radial distribution functions generated by *MD* (solid lines) and *PY* (squares) at $T = 0.722$ and $\rho = 0.8442$. $N = 256$ in the MD simulations.

where,

$$f(r) = 1 - \exp(-\alpha r), \tag{9}$$

The arbitrary parameter, α, has an optimum value, $\sim 1/2$,[15] and it was set to 1/2 in this study. We have,

$$g(r) = \exp(-\beta\phi(r))\left(1 + \frac{\exp(\gamma(r)f(r)) - 1}{f(r)}\right). \tag{10}$$

The properties of interest are the internal energy E and the pressure P,

$$E/(k_B T) = 3/2 + \frac{2\pi\rho}{k_B T}\int_0^\infty g(r)r^2\phi(r)dr, \tag{11}$$

$$PV/Nk_B T = 1 - \frac{2\pi\rho}{3k_B T}\int_0^\infty g(r)r^3\phi'(r)dr, \tag{12}$$

$$\begin{aligned}\chi_T^{-1} &= \\ &= \left[\frac{\partial P}{\partial p}\right]_T \Big/ (k_B T), \\ &= 1/S(0), \\ &= 1 - 4\pi\rho\int_0^\infty drr^2 c(r).\end{aligned} \tag{13}$$

Downloaded At: 08:33 28 January 2011

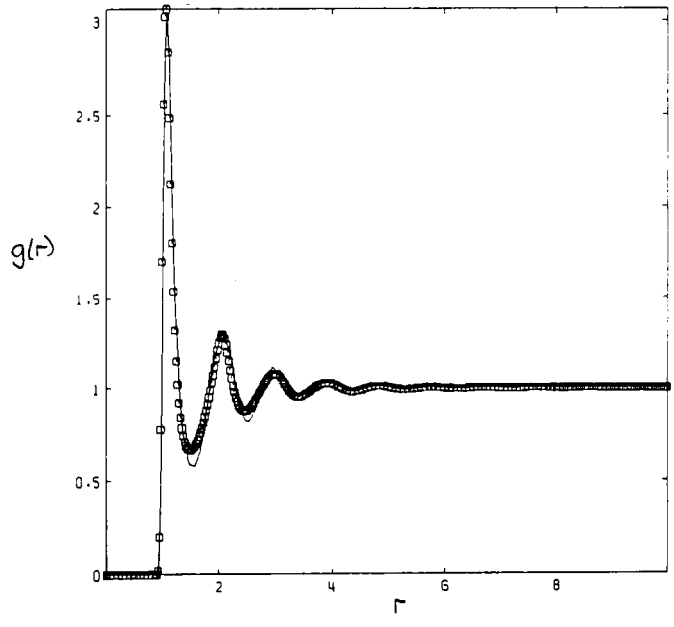

Figure 5 Comparison between the pair radial distribution functions generated by *MD* (solid lines) and *HNC* (squares) at $T = 0.722$ and $\rho = 0.8442$. $N = 256$ in the MD simulations.

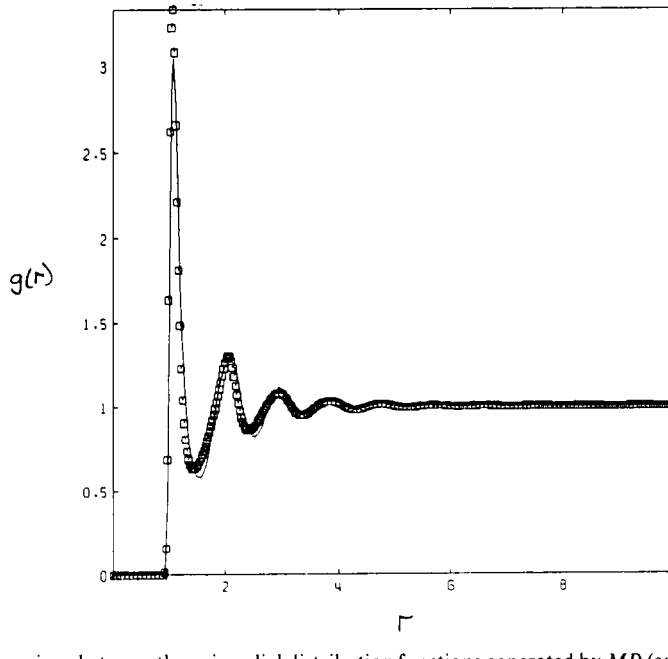

Figure 6 Comparison between the pair radial distribution functions generated by *MD* (solid lines) and *RY* (squares) at $T = 0.722$ and $\rho = 0.8442$. $N = 256$ in the MD simulations.

Downloaded At: 08:33 28 January 2011

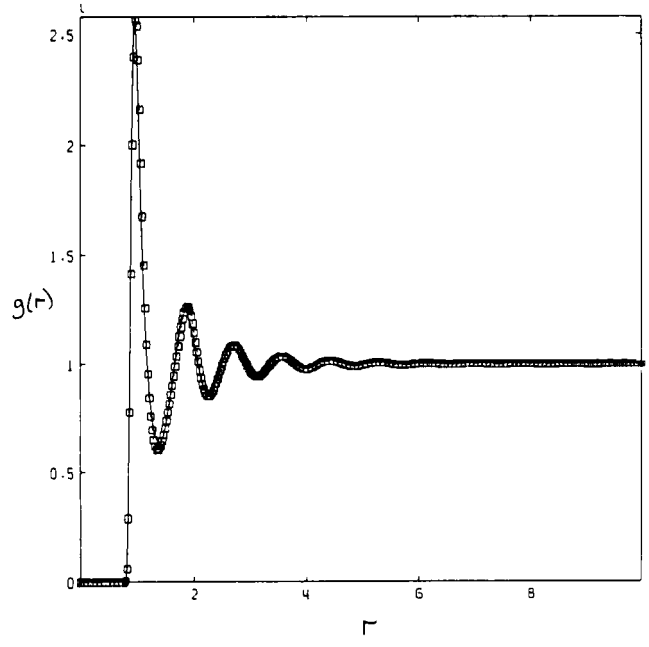

Figure 7 Comparison between the pair radial distribution functions generated by *MD* (solid lines) and *PY* (squares) at $T = 6.0$ and $\rho = 1.18$. $N = 256$ in the MD simulations.

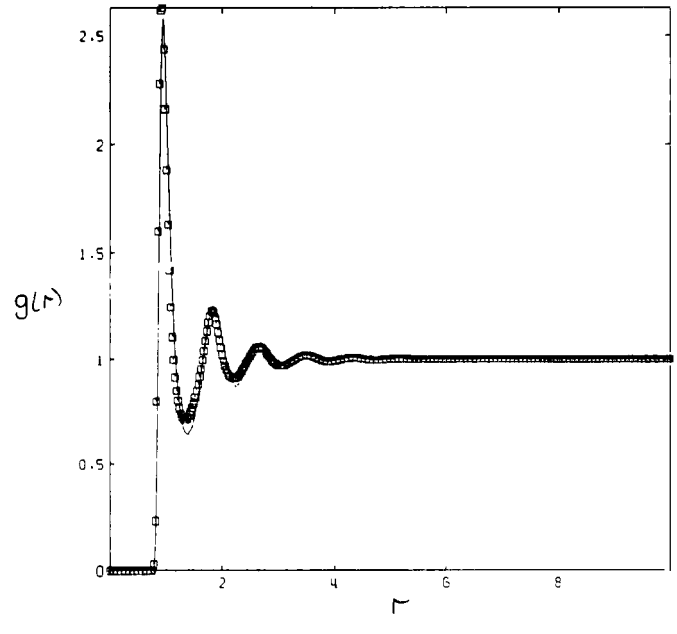

Figure 8 Comparison between the pair radial distribution functions generated by *MD* (solid lines) and *HNC* (squares) at $T = 6.0$ and $\rho = 1.18$. $N = 256$ in the MD simulations.

Downloaded At: 08:33 28 January 2011

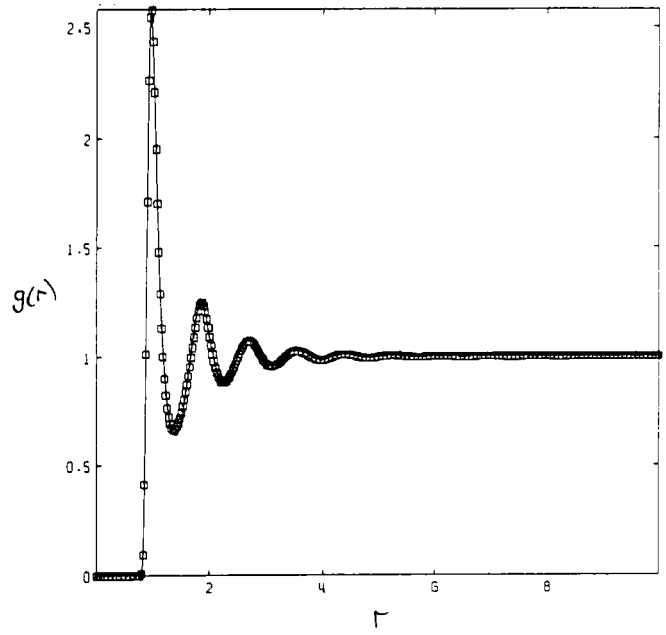

Figure 9 Comparison between the pair radial distribution functions generated by *MD* (solid lines) and *RY* (squares) at $T = 6.0$ and $\rho = 1.18$. $N = 256$ in the MD simulations.

Alternatively,

$$\chi_T = 1 + 4\pi\rho \int_0^\infty r^2 h(r) dr. \tag{14}$$

The infinite frequency shear and bulk moduli are expressible in terms of the potential energy components reduced from the expressions of Zwanzig and Mountain[16,17]. For the infinite-frequency shear modulus, G_∞,

$$G_\infty = \rho k_B T + \frac{2\pi\rho^2}{15} \int_0^\infty dr g(r) \frac{d}{dr}\left(r^4 \frac{d\phi}{dr}\right), \tag{15}$$

For the infinite-frequency compressional modulus, K_∞,

$$K_\infty = \frac{2}{3}\rho k_B T + P + \frac{2\pi\rho^2}{9} \int_0^\infty dr g(r) r^3 \frac{d}{dr}\left(r \frac{d\phi}{dr}\right). \tag{16}$$

The particles in a Lennard-Jones fluid interact via a pair potential, $\phi(r)$,

$$\phi(r) = 4\varepsilon((\sigma/r)^{12} - (\sigma/r)^6). \tag{17}$$

The moduli can be reduced to the following simple expressions for the LJ fluid,

$$G_\infty = \rho k_B T + \rho(108\Phi_{12} + 18\Phi_6)/15, \tag{18}$$

Downloaded At: 08:33 28 January 2011

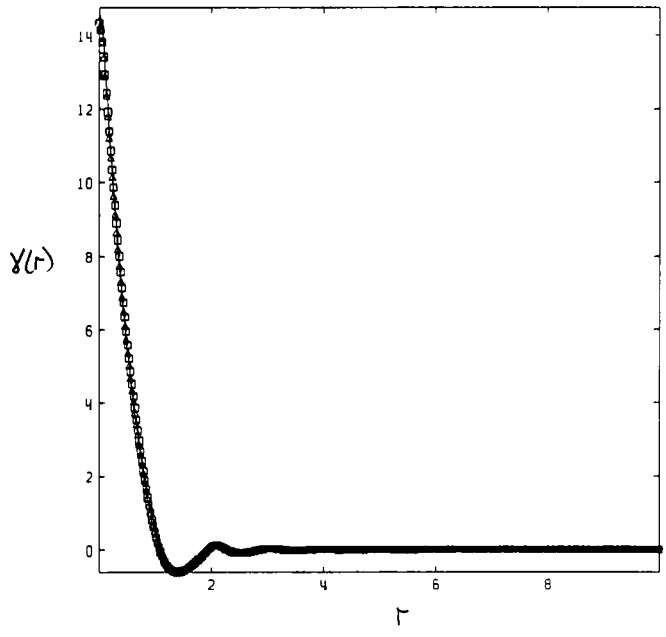

Figure 10 Comparison between the $\gamma(r)$ obtained by the different closure relations: PY (solid line), HNC (squares) and RY (triangles), $T = 1.06$ and $\rho = 0.731$.

Downloaded At: 08:33 28 January 2011

where Φ_{12} and Φ_6 are the r^{-12} and r^{-6} components of Φ, the configurational energy per particle ($E = 3k_BT/2 + \Phi$). Similarly for the bulk compressional modulus,

$$K_\infty = 5\rho k_B T/3 + \rho(20\Phi_{12} + 6\Phi_6). \tag{19}$$

2 THE INTEGRAL EQUATION ALGORITHM

The standard Picard/Broyles method was used to solve Eqs. (1)–(3) coupled with a particular choice of the closure relationship. We will consider the PY closure of Eq. (4) specifically but the procedure is common to them all. Substituting Eq. (3) in Eq. (1) we have,

$$\gamma(r) = \rho \int d\underline{r}' c(|\underline{r} - \underline{r}'|)[\gamma(\underline{r}') + c(\underline{r}')], \tag{20}$$

Now if we define the following Fourier transforms,

$$\hat{c}(k) = \int c(\underline{r})\exp(i\underline{k}\cdot\underline{r})d\underline{r}$$

$$= \frac{4\pi}{k}\int_0^\infty rc(r)\sin(kr)dr, \tag{21}$$

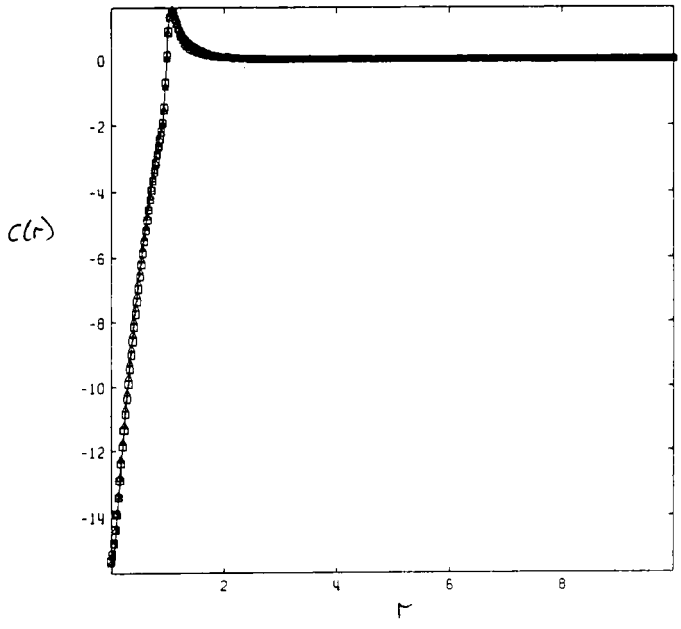

Figure 11 Comparison between the $c(r)$ obtained by the different closure relations: PY (solid line), HNC (squares) and RY (triangles), $T = 1.06$ and $\rho = 0.731$.

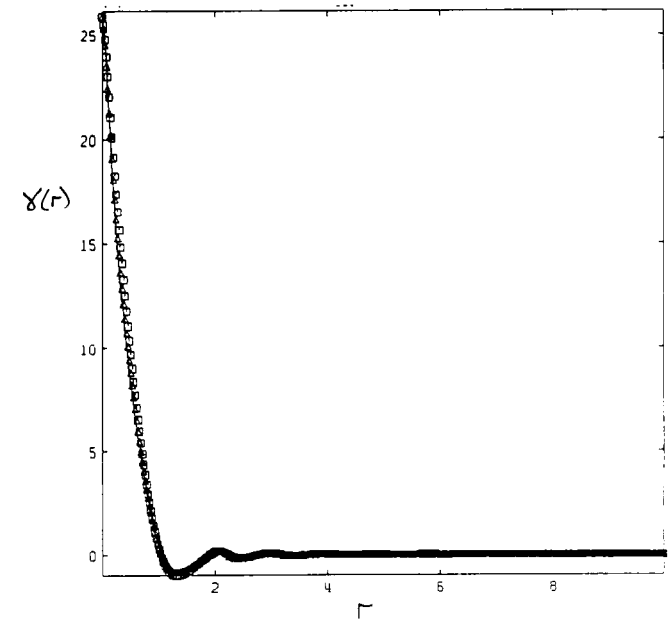

Figure 12 Comparison between the $\gamma(r)$ obtained by the different closure relations: PY (solid line), HNC (squares) and RY (triangles), $T = 0.722$ and $\rho = 0.8442$.

Downloaded At: 08:33 28 January 2011

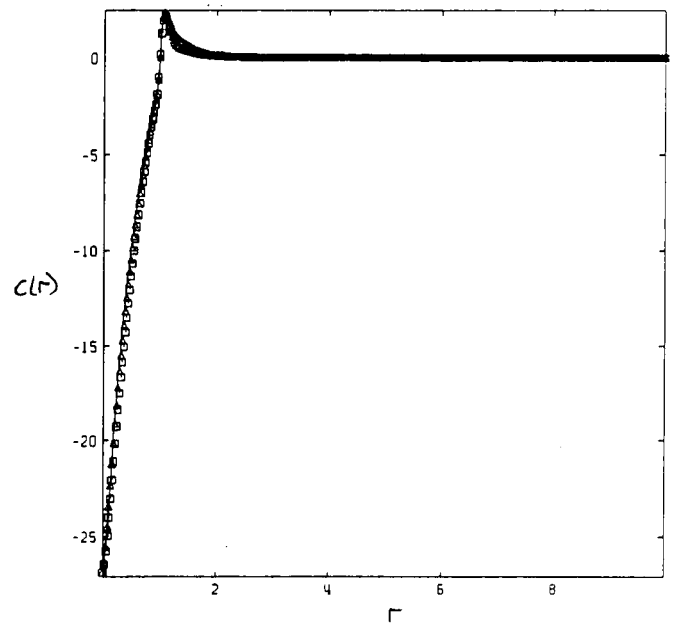

Figure 13 Comparison between the $c(r)$ obtained by the different closure relations: PY (solid line), HNC (square) and RY (triangles), $T = 0.722$ and $\rho = 0.8442$.

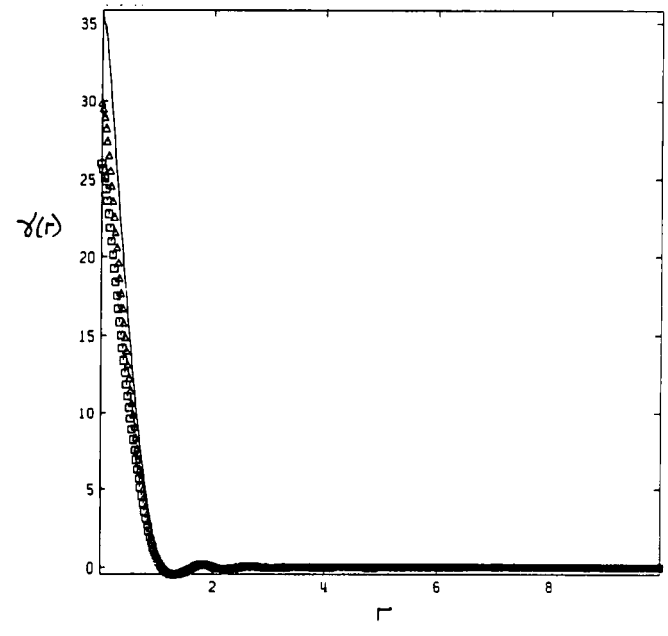

Figure 14 Comparison between the $\gamma(r)$ obtained by the different closure relations: PY (solid line), HNC (squares) and RY (triangles), $T = 6.0$ and $\rho = 1.18$.

Downloaded At: 08:33 28 January 2011

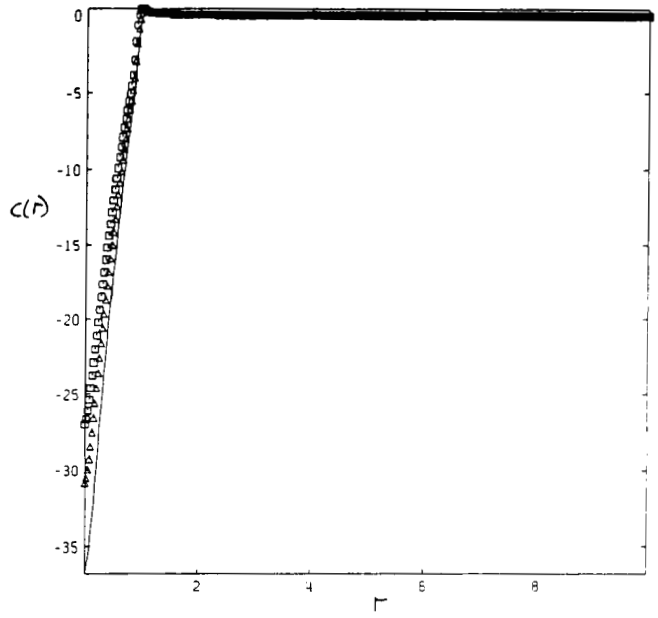

Figure 15 Comparison between the $c(r)$ obtained by the different closure relations: PY (solid line), HNC (squares) and RY (triangles), $T = 6.0$ and $\rho = 1.18$.

and,

$$\hat{\gamma}(k) = \int \gamma(\underline{r})\exp(i\underline{k}\cdot\underline{r})d\underline{r}$$

$$= \frac{4\pi}{k}\int_0^\infty r\gamma(r)\sin(kr)dr, \tag{22}$$

then,

$$\hat{\gamma} = \rho\hat{c}\hat{\gamma} + \rho\hat{c}\hat{c}, \tag{23}$$

The $\hat{\gamma}$ can be Fourier transformed from k space to r space,

$$\gamma(r) = \left(\frac{1}{2\pi}\right)^3 \int \hat{\gamma}(\underline{k})\exp(-i\underline{k}\cdot\underline{r})d\underline{k}$$

$$= \frac{1}{2\pi^2 r}\int_0^\infty k\gamma(\hat{k})\sin(kr)dr, \tag{24}$$

The cycle is completed by substituting the result of Eq. (24) back into the PY closure relationship,

$$c(r) = (1 + \gamma(r))(\exp(-\beta\phi(r)) - 1), \tag{25}$$

For HNC Eq. (6) would be used instead and for RY Eq. (8) would be used. The cycle starting from Eq. (21) is repeated until convergence is reached.

Downloaded At: 08:33 28 January 2011

The technical details are as follows. The distance range covered is partitioned into N intervals, Δr, $r_i = i\Delta r$. Similarly, for k-space, $k_i = 2\pi i/(N\Delta r)$, therefore $r_j k_j = 2\pi ij/N$. All $r-$ and k-dependent functions are evaluated at r and k intervals as follows,

$$\begin{aligned} c_i &= (1 + \gamma_i)(\exp(-\beta\phi_i) - 1), i \leq N/2 \\ &= 0, i > N/2 \end{aligned} \tag{26}$$

$$c_i^n = c_i, \tag{27}$$

$$\hat{c}_j = \frac{4\pi\Delta r}{k_j} \sum_{i=1}^{N/2-1} r_i c_i \sin(k_j r_i), \tag{28}$$

$$\hat{\gamma}_j = \rho \frac{\hat{c}_j^2}{(1 - \rho\hat{c}_j)}, \tag{29}$$

$$\gamma_i' = \frac{\Delta k}{2\pi^2 r_i} \sum_{j=1}^{N/2-1} k_j \hat{\gamma}_j \sin(k_j r_i), \tag{30}$$

where $\Delta k = 2\pi/(N\Delta r)$,

$$\begin{aligned} c_i' &= (1 + \gamma_i')(\exp(-\beta\phi_i) - 1), i \leq N/2 \\ &= 0, i > N/2. \end{aligned} \tag{31}$$

At high density we facilitate convergence by 'mixing in' a certain fraction of the old direct correlation function, c_i^n, with the 'new' function, c_i',

$$c_i = \delta c_i^n + (1 + \delta)c_i', \tag{32}$$

with a value of $\delta = 0.5$ being typical. This damps down oscillations between consecutive iterations. It was found not necessary to resort to the Gillan Method[4] to achieve the objectives of this work. The convergence criterion was,

$$\sum_{i=1}^{N} (\gamma_i' - \gamma_i)^2 \leq \varepsilon, \tag{33}$$

choosing $\varepsilon = 10^{-3}$. Equation (27) is now returned to and the cycle to equation (33) is repeated. Here, $N = 1600$ and $\Delta r = 0.025\sigma$.

It is worth noting that even at the densest states convergence only takes $\sim$ several minutes on a microcomputer making use of Discrete Fourier Transform (NAG) library routines. Implementation of the integral equations is significantly easier than 20–30 years ago when these equations were first solved numerically. Computations were carried out on a VAX 11/780 at the Royal Holloway & Bedford New College Computer Centre.

Downloaded At: 08:33 28 January 2011

3 THE MD METHOD

The basic technique for simulating the LJ molecules has been described elsewhere[18,19]. The MD simulations were performed on a cubic unit cell of volume V containing $N = 256$ Lennard-Jones (LJ) particles of mass, m. The interactions were truncated at $r_c = 2.5\sigma$. A large time step version of the Verlet algorithm was used to increment the positions of the molecules[20]. We use LJ reduced units throughout, e.g., $k_B T/\varepsilon \to T$, and number density, $\rho = N\sigma^3/V$. The moduli are in $\varepsilon\sigma^{-3}$. The temperature was fixed by the Gaussian isokinetic scheme[20].

4 RESULTS AND DISCUSSION

A summary of the properties from Eqs. (11) to (19) is presented in Table 1. These are compared with simulation and LJ simulation-fitted equation of state predictions for the same quantities. All states are in the fluid phase. The equation of state internal energy agrees better than the pressure with the integral equation predictions, as noted elsewhere[13]. Table 1 reveals that at low to intermediate densities all three closures give good agreement with 'exact' (simulation) values for the elastic moduli. Agreement is usually within 2–3%, being slightly better for PY than HNC or RY. Close to the solid phase boundary these integral equations are severely tested because many-body correlations start to increase in complexity. (In the low density limit the two-body distribution function, $g(r)$, suffices to account for all physical properties.) At high temperature ($\gg T_c$), the RY closure gives by far the most superior agreement with the simulation moduli. It is significantly better than PY or HNC. The 2–3% agreement with the simulation values is maintained. The PY underestimates the elastic moduli by $\sim 10\%$ and the HNC overestimates the moduli by $\sim 10\%$.

The most severe test of these integral equations is at high density (near the maximum liquid density) and low temperature (below the critical temperature (≈ 1.3)). We note that all closure relationships overestimate the elastic moduli by 5–10%.

For the first time fluid structure integral equations have been used to predict the elastic moduli of the Lennard-Jones fluid over an appreciable region of the phase diagram. Perhaps the main conclusion to come out of these calculations and MD simulations is that the closure of Rogers and Young provides startlingly good elastic (and thermodynamic quantities) at high density and temperature. It is recommended in studies of the elastic moduli of sterically stabilised dense suspensions where the colloidal particle interactions are essentially repulsive.

Acknowledgements

D.M.H. gratefully thanks *The Royal Society* for the award of a *Royal Society 1983 University Research Fellowship*. Dr. W. Smith (TCS, S.E.R.C. Daresbury Laboratory) is thanked for helpful discussions concerning Fast Fourier Transforms. The award of computer time to perform the simulations from the S.E.R.C. at the University of London Computer Centre is gratefully acknowledged.

Downloaded At: 08:33 28 January 2011

Downloaded At: 08:33 28 January 2011

Table 1 The MD LJ moduli G_∞ and K_∞ compared with the predictions from the Ree[22] (res) and Nicholas *et al.*[21] (nes) equations of state, using the pressure and internal energy. PY, HNC and RY denote the solutions from the Percus-Yevick, Hypernetted chain and Rogers-Young closures. The moduli in brackets are from independent MD simulations.

Method	T	ρ	E/kT	PV/NkT	χ_T	G_∞	G_∞-*MD*	K_∞	K_∞-*MD*
res	1.4562	0.3	0.196	0.453	9.56	2.46		4.49	
nes	1.4562	0.3	0.083	0.452	5.09	2.69		4.88	
PY	1.4562	0.3	0.055	0.501	3.98	2.81	(2.71)	4.25	(4.06)
HNC	1.4562	0.3	0.043	0.493	6.08	2.83		4.27	
RY	1.4562	0.3	0.047	0.492	5.12	2.82		4.25	
res	1.4562	0.5249	−0.839	0.482	0.60	8.16		14.34	
nes	1.4562	0.5249	−0.891	0.476	0.68	8.34		14.62	
PY	1.4562	0.5249	−0.898	0.744	0.69	8.98	(8.46)	14.57	(13.37)
HNC	1.4562	0.5249	−0.887	0.803	0.86	9.07		14.82	
RY	1.4562	0.5249	−0.893	0.766	0.77	9.01		14.66	
res	1.4562	0.863	−2.234	3.855	0.045	34.54		67.51	
nes	1.4562	0.863	−2.224	3.784	0.045	34.21		66.53	
PY	1.4562	0.863	−2.214	4.148	0.064	35.53	(34.09)	67.12	(63.64)
HNC	1.4562	0.863	−1.939	5.622	0.085	39.43		77.33	
RY	1.4562	0.863	−2.115	4.671	0.073	36.90		70.73	
res	1.4562	1.0017	−2.413	7.974	0.021	59.37		122.22	
nes	1.4562	1.0017	−2.424	7.812	0.022	58.74		120.69	
PY	1.4562	1.0017	−2.514	7.504	0.029	58.03	(58.15)	115.69	(116.27)
HNC	1.4562	1.0017	−1.876	10.790	0.045	67.94		141.79	
RY	1.4562	1.0017	−2.279	8.730	0.035	61.74		125.46	
res	2.6974	0.4	0.619	1.178	0.510	6.22		12.91	
nes	2.6974	0.4	0.620	1.165	0.532	6.17		12.80	
PY	2.6974	0.4	0.619	1.228	0.519	6.38	(6.22)	11.12	(10.75)
HNC	2.6974	0.4	0.624	1.262	0.555	6.46		11.33	
RY	2.6974	0.4	0.621	1.234	0.540	6.39		11.16	
res	2.6974	0.6993	0.032	2.604	0.115	24.26		50.26	
nes	2.6974	0.6993	0.036	2.531	0.117	23.81		49.23	
PY	2.6974	0.6993	0.035	2.612	0.134	24.27	(23.98)	46.53	(45.88)
HNC	2.6974	0.6993	0.127	3.181	0.159	26.66		56.65	
RY	2.6974	0.6993	0.066	2.780	0.146	25.04		48.52	

Downloaded At: 08:33 28 January 2011

res	2.6974	0.9534	−0.132	6.290	0.037	63.53		138.24	
nes	2.6974	0.9534	−0.124	6.225	0.037	62.93		136.90	
PY	2.6974	0.9534	−0.262	5.399	0.045	58.26	(62.70)	119.73	(131.16)
HNC	2.6974	0.9534	0.187	7.924	0.061	72.20		155.94	
RY	2.6974	0.9534	−0.090	6.434	0.050	64.13		134.83	
res	2.6974	1.06	0.012	9.048	0.024	92.31		205.60	
nes	2.6974	1.06	0.020	8.976	0.024	91.59		203.99	
PY	2.6974	1.06	0.279	7.255	0.029	80.94	(91.87)	170.67	(198.86)
HNC	2.6974	1.06	0.520	11.587	0.042	107.13		239.09	
RY	2.6974	1.06	−0.003	8.817	0.024	90.54		195.60	
res	6.0	0.9355	1.1841	5.2998	0.057	86.53		203.71	
nes	6.0	0.9355	1.1811	5.2259	0.057	85.37		200.94	
PY	6.0	0.9355	1.1442	5.1011	0.052	84.26	(85.10)	186.47	(189.12)
HNC	6.0	0.9355	1.3671	6.1671	0.079	96.20		218.34	
RY	6.0	0.9355	1.1965	5.3055	0.066	86.29		192.15	
res	6.0	1.18	1.6860	9.7168	0.0265	185.90		447.43	
res	6.0	1.18	1.6748	9.6442	0.0265	184.74		444.47	
PY	6.0	1.18	1.3642	8.0525	0.0249	161.49	(183.44)	369.01	(427.21)
HNC	6.0	1.18	2.1672	11.980	0.0405	217.62		518.18	
RY	6.0	1.18	1.6045	9.2282	0.0321	178.29		413.67	
res	1.06	0.731	−3.2348	0.5316	0.1135	17.30		29.65	
nes	1.06	0.731	−3.2815	0.5722	0.1166	17.56		30.16	
PY	1.06	0.731	−3.2020	1.5244	0.2015	19.48	(17.43)	33.28	(28.31)
HNC	1.06	0.731	−3.1278	1.7687	0.2688	19.77		34.15	
RY	1.06	0.731	−3.1744	1.5674	0.2352	19.48		33.35	
res	1.06	0.848	−3.9190	2.5023	0.0449	28.33		51.72	
nes	1.06	0.848	−3.9230	2.4499	0.0468	28.21		51.42	
PY	1.06	0.848	−3.8438	3.2598	0.086	30.049	(28.14)	54.14	(49.42)
HNC	1.06	0.848	−3.6124	4.5131	0.10424	32.431		60.367	
RY	1.06	0.848	−3.7547	3.8003	0.0918	31.122		56.905	
res	0.722	0.8442	−6.9126	0.1964	0.043	23.75		39.83	
nes	0.722	0.8442	−6.9265	0.1944	0.050	23.79		39.89	
PY	0.722	0.8442	−6.6850	2.7691	0.125	27.79	(23.76)	48.49	(38.56)
HNC	0.722	0.8442	−6.5669	2.7365	0.164	27.39		47.76	
RY	0.722	0.8442	−6.6330	2.7733	0.142	27.65		48.24	

References

1. J.-P. Hansen and I. R. McDonald, *Theory of Simple Liquids*, (Academic Press, London, 1986).
2. D. M. Heyes, *Phys. Rev. B*, **37**, 5677 (1988).
3. D. M. Heyes, *J. Chem. Soc. Faraday Trans II*, in press.
4. M. J. Gillan, *Mol. Phys.*, **38**, 1781 (1979).
5. F. Mandel, R. J. Bearman and M. Y. Bearman, *J. Chem. Phys.*, **52**, 3315 (1970).
6. F. Mandel and R. J. Bearman, *J. Chem. Phys.*, **50**, 4121 (1969).
7. R. O. Watts, *J. Chem. Phys.*, **50**, 4122 (1969).
8. A. A. Broyles, *J. Chem. Phys.*, **35**, 493 (1961).
9. R. O. Watts, *J. Chem. Phys.*, **47**, 2709 (1969).
10. D. Levesque, *Physica*, **32**, 1985 (1966).
11. J. A. Barker and D. Henderson, *Ann. Rev. Phys. Chem.*, 439 (1972).
12. F. Gallerani, G. L. Vecchio and L. Reatto, *Phys. Rev. A*, **32**, 2526 (1985).
13. J. A. Barker, D. Henderson and R. O. Watts, *Phys. Lett.*, **31A**, 48 (1970).
14. J. A. Barker and D. Henderson, *Rev. Mod. Phys.*, **48**, 587 (1976).
15. F. J. Rogers and D. A. Young, *Phys. Lett.* **102A**, 303 (1984).
16. R. Zwanzig and R. D. Mountain, *J. Chem. Phys.*, **43**, 4464 (1965).
17. M. J. Grimson, *Mol. Phys.*, **59**, 737 (1986).
18. D. M. Heyes, *J. Chem. Soc., Faraday Trans. II*, **83**, 1985 (1987).
19. K. D. Hammonds and D. M. Heyes, *J. Chem. Soc. Faraday Trans.* 2, **84**, 705 (1988).
20. D. MacGowan and D. M. Heyes, *Mol. Sim.*, **1**, 277, (1988).
21. J. J. Nicholas, K. E. Gubbins, W. B. Street, and D. J. Tildesley, *Mol. Phys.*, 1979, **37**, 1429.
22. F. H. Ree, *J. Chem. Phys*, 1980, **73**, 5401.

Downloaded At: 08:33 28 January 2011